Biochemical and Biophysical Research Communications 434 (2013) 614–619

Contents lists available at SciVerse ScienceDirect

Biochemical and Biophysical Research Communications

journal homepage: www.elsevier.com/locate/ybbrc

Conformational changes induced in the eukaryotic translation initiation factor eIF4E by a clinically relevant inhibitor, ribavirin triphosphate

Laurent Volpon [a,1], Michael J. Osborne [a,1], Hiba Zahreddine [a], Andrea A. Romeo [b], Katherine L.B. Borden [a,*]

[a] Institute of Research in Immunology and Cancer (IRIC), Department of Pathology and Cell Biology, Université de Montréal, Pavilion Marcelle-Coutu, Chemin Polytechnique, Montreal, Qc, Canada H3T 1J4
[b] Aegera Therapeutics (Pharmascience Inc.), 810 Chemin du golf, Verdun, Montreal, Qc, Canada H3E 1A8

ARTICLE INFO

Article history:
Received 21 March 2013
Available online 10 April 2013

Keywords:
NMR
Ribavirin
Methyl 7-guanosine (m^7G) cap
Drug design

ABSTRACT

The eukaryotic translation initiation factor eIF4E is highly elevated in human cancers including acute myeloid leukemia (AML). A potential anticancer agent, ribavirin, targets eIF4E activity in AML patients corresponding to clinical responses. To date, ribavirin is the only direct inhibitor of eIF4E to reach clinical trials. We showed that ribavirin acts as a competitive inhibitor of the methyl 7-guanosine (m^7G) cap, the natural ligand of eIF4E. Here we examine the conformational changes occurring in human eIF4E upon binding the active metabolite of ribavirin, ribavirin triphosphate (RTP). Our NMR data revealed an unexpected concentration dependence on RTP affinity for eIF4E. We observed NMR spectra characteristic of tight binding at low micromolar concentrations (2–5 μM eIF4E) but much weaker affinity at more typical NMR concentrations (50–200 μM). Comparison of chemical shift perturbation and line broadening suggest that the two eIF4E-RTP complexes differ in the precise positioning of RTP within the cap binding pocket, with the high affinity complex showing more extensive changes to the central β-sheet and dorsal surface of eIF4E, similar to m^7G cap. The differences between high and low affinity complexes arise due to concentration dependent aggregation of eIF4E and RTP. Given the intracellular concentrations of eIF4E and RTP and the differential binding toward the W56A eIF4E mutant the high affinity complex is the most physiologically relevant. In summary, these findings demonstrate that RTP binds in the cap-binding site but also suggests new features of this pocket that should be considered in drug design efforts and reveal new insights into ligand eIF4E recognition.

1. Introduction

The eukaryotic translation initiation factor eIF4E is overexpressed in about 30% of human cancers [1,2]. eIF4E modulates the expression of transcripts involved in proliferation and survival by modulating their mRNA export and translation [1,2]. In both cases, eIF4E must associate with the methyl-7 guanosine (m^7G) cap structure on the 5′ end of mRNAs [1–3]. NMR and X-ray crystal structures indicate that the m^7G cap intercalates between two tryptophan residues (W56 and W102) which recognize the m^7G moiety [4–6]. The cap-binding pocket also includes other residues such as W166 which contacts the m^7G as well as positively charged residues (R157 and K162) representing the phosphate binding site. This cap-binding activity of eIF4E is required for its ability to oncogenically transform cells [7]. In cancers with elevated eIF4E, the cells develop an oncogene addiction or dependency on eIF4E [8,9]. This provides a therapeutic window for targeting eIF4E in patients.

The activity of eIF4E has been targeted in poor prognosis acute myeloid leukemia (AML) patients with ribavirin, a competitive inhibitor of m^7G cap [9–11]. Targeting of eIF4E activity in a Phase II clinical trial correlated with clinical responses including 1 complete remission, 2 partial remissions, 2 blast responses (50+% reduction in leukemia blast count) and 6 patients with stable disease reported in the original 11 evaluable patients [10]. For comparison targeting the mTOR pathway via the 4E-BP1 inhibitor, rapamycin led to 0 out of 22 responses in a similar patient population [10].

In cells, ribavirin antagonized the ability of eIF4E to export or translate target transcripts with an indistinguishable profile from

Abbreviations: AML, acute myeloid leukemia; RTP, ribavirin triphosphate; mTOR, mammalian target of rapamycin; CD, circular dichroism; m^7G, 7-methyl-guanosine; m^7GTP, 7-methyl-guanosine-5′-triphosphate; HSQC, heteronuclear single quantum coherence; RING, really interesting new gene; PML, promyelocytic leukemia; ITC, isothermal calorimetry.

* Corresponding author. Address: Institute of Research in Immunology and Cancer (IRIC), Université de Montréal, Pavilion Marcelle-Coutu, 2950, Chemin Polytechnique, Montreal, Qc, Canada H3T 1J4. Fax: +1 (514) 343 7379.
E-mail address: katherine.borden@umontreal.ca (K.L.B. Borden).

[1] These authors contributed equally to this work.

0006-291X/$ - see front matter © 2013 Elsevier Inc. All rights reserved.
http://dx.doi.org/10.1016/j.bbrc.2013.03.125

RNAi-mediated knockdown of eIF4E [9,10,12]. As expected, ribavirin inhibited eIF4E-mediated oncogenic transformation in cell and animal models as well as in AML patients [9,12]. The active metabolite in cells is ribavirin triphosphate (RTP) [13]. Multiple biophysical studies showed that RTP and ribavirin directly bind to eIF4E with a similar affinity as cap [9,11]. Mutation of the cap-binding site (W56A) reduced ribavirin binding by nearly 15-fold similar to effects for the cap [9,10]. The eIF4E-RTP complex was studied in different solution conditions including at 0.2 μM eIF4E protein in 10 mM sodium phosphate, pH 7.5, 150 mM NaCl, or by mass spectrometry at 20 μM eIF4E in 5% aqueous acetonitrile, 20 mM ammonium acetate (pH 6.5) [11]. Complexes were not detected in 20 mM HEPES, 0.2 mM EDTA, 100 mM KCl, pH 8.0 [11] where substantial aggregation is observed relative to phosphate buffers.

The structural changes induced in eIF4E by RTP binding are unknown. A better understanding of how RTP binds is necessary for future drug design efforts. Here, we demonstrate that RTP and m^7GTP induce changes in eIF4E upon binding while GTP does not have these effects, as observed by circular dichroism (CD). Chemical shift mapping of ^1H–^{15}N HSQC NMR experiments were used to monitor eIF4E-RTP complexes as a function of eIF4E concentrations ranging from 2 to 200 μM. These NMR data showed that increasing eIF4E concentrations led to weaker affinities for RTP. This affinity dependence was concomitant with aggregation of eIF4E and RTP. Chemical shift mapping of the amide NMR resonances in the high and low affinity eIF4E–RTP complexes show similar but, importantly, different perturbations at or surrounding the cap-binding site suggesting that the precise molecular contacts underlying the high and low affinity eIF4E–RTP complexes are distinct.

2. Materials and methods

Human eIF4E was purified as described previously [6]. The absence of any cap was verified as described in the Supplementary methods and Supplementary Fig. 1A. ^1H–^{15}N HSQC spectra were collected in 10 mM sodium phosphate, 150 mM NaCl, pH 7.5 and 20 °C on a 600 MHz Varian Inova spectrometer equipped with a HCN coldprobe. Other materials and methods are given in the Supplementary data.

3. Results

3.1. RTP, but not GTP, induces changes in the secondary structure of eIF4E

Far ultraviolet (UV) circular dichroism (CD) has shown that eIF4E undergoes a detectable change in its peptide backbone conformation upon m^7GTP binding [7,14,15]. We therefore monitored the changes in molar ellipticity by far UV CD of eIF4E upon addition of RTP, GTP and m^7GTP. In contrast to RTP or m^7GTP where changes are observed upon addition of ~20:1 molar ratio, GTP induced no changes in molar ellipticity (Fig. 1). The extent of conformational change observed is consistent with previous observations [14,15]. Thus eIF4E binds both m^7GTP and RTP, but not GTP. These data correlate with our previous cap chromatography experiments showing that GTP did not compete for eIF4E bound to a cap column while RTP and m^7GTP did [11].

3.2. NMR studies of the eIF4E–RTP complex

To understand the molecular basis of RTP binding to eIF4E we used NMR chemical shift mapping studies. Spectral changes induced by RTP addition as a function of concentration for human eIF4E (2–200 μM) were monitored using ^1H–^{15}N HSQC experiments. Experiments within 2–5 μM eIF4E, where 2 μM was our lowest limit of detection, were chosen based on our CD and previous biophysical studies. Given the 6–10 days required for acquisition of the HSQC at low eIF4E concentration, the integrity of apo-eIF4E was checked before and after acquisition by SDS–PAGE with no detectable degradation over this time period.

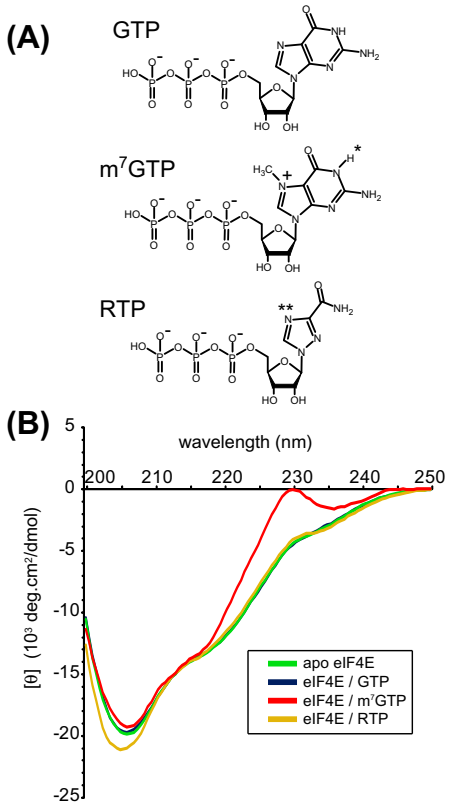

Fig. 1. Analysis of RTP binding and protein samples. (A) The chemical structures of GTP, m^7GTP and RTP. $*$ denotes proton that partially dissociate at pH 7.2 and $**$ denotes where protonation would cause a positive charge on the free triazole. (B) Circular dichroism spectra in the far ultraviolet upon addition of GTP, m^7GTP or RTP to human eIF4E.

3.3. eIF4E exhibits a concentration dependent affinity for RTP

Example ^1H–^{15}N HSQC spectra recorded for eIF4E in the absence and presence of RTP at low eIF4E concentrations (2–5 μM) and high eIF4E concentrations (50–200 μM) are shown in Figs. 2A and 3A, respectively. These data reveal two complexes in different exchange regimes on the NMR timescale, signifying different affinities for RTP. At high eIF4E concentrations we observed peaks in fast exchange consistent with a weak affinity for RTP. In contrast, the low concentration eIF4E sample (2 μM) exhibited loss of peaks and in some cases, appearance of new peaks upon addition of RTP at ~20-fold excess. These spectra indicate the low concentration eIF4E–RTP complex is in intermediate to slow exchange, consistent with affinities detected for this complex from previous biophysical studies (K_d of 0.13 μM [9]). For the low concentration complex with 40 μM RTP, it is important to note this concentration is readily achievable in patients with no toxicity [10,16]. Importantly, many regions of the protein did not undergo detectable changes in either complex indicating the effects of RTP are specific.

3.4. Chemical shift mapping reveals distinct complexes at high and low eIF4E concentrations

Mapping of the spectral changes onto the eIF4E structure indicates that a similar set of residues are perturbed in both complexes

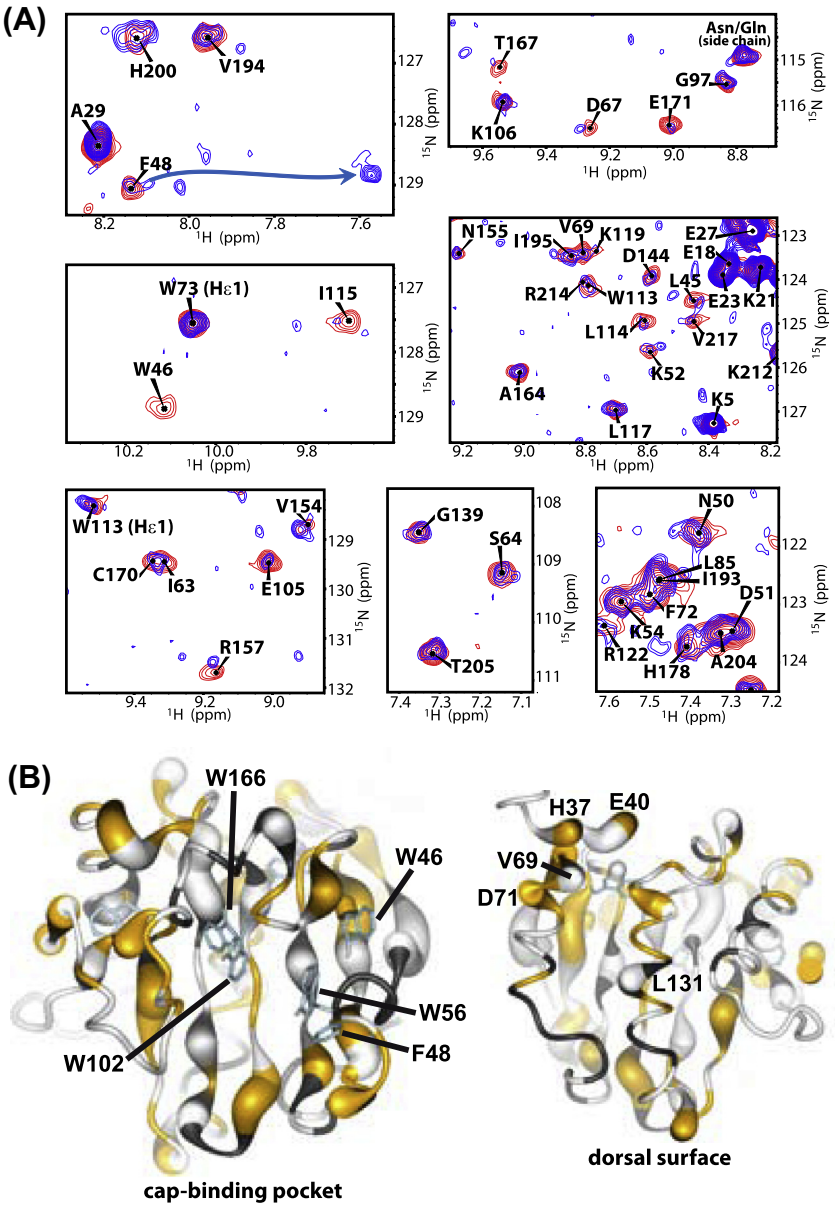

Fig. 2. NMR analysis of the low micromolar eIF4E–RTP complex is characterized by intermediate and slow exchange. (A) Regions highlighting specific residues of ^{1}H–^{15}N HSQC spectra of apo eIF4E (red) with ~20-fold molar excess of RTP (blue). Representative result is shown that was repeated independently three times. Spectra were normalized to W73 indole (middle left panel). (B) Line broadening was mapped as the width of the tube onto the structure of the cap bound eIF4E [28] (pdb code: 3AM7) where gold indicates a RTP induced shift relative to apo, white is no shift and black is unknown due to spectral overlap. Two views are shown, the cap (left panel) binding site and the helical dorsal surface (right panel).

(Figs. 2B, 3B and Supplementary Fig. 2C and D). These residues (colored cyan in Fig. 4A) are centered around the cap binding pocket, including the β-strands at the bottom of the cap-binding pocket (e.g. β-strands 1 and 4–6), the phosphate binding region (R157 and K162) as well as the surface loops important for m^{7}G cap binding. A substantial number of resonances, however, are perturbed differentially indicating the high and low affinity complexes have distinct binding modes (dark blue and green in Fig. 4A). For instance, while the N50 and T205 (Fig. 3) are among the most affected residues in the low affinity complex, these are not altered in the high affinity complex (Fig. 2). One of the most striking changes in the high affinity complex involves F48 (adjacent to W56 in the eIF4E structure, Fig. 2B), which undergoes broadening with a new peak found at almost the exact position of the F48 cross peak corresponding to the m^{7}GTP bound form of eIF4E (see the arrow in Fig. 2A). In the low affinity complex the F48 peak is only minimally perturbed relative to apo-eIF4E. Similarly, many peaks that disappear in the high affinity complex are not affected in the low affinity complex, e.g. I115, T167, K52 among others (compare Figs. 2A and 3A).

Mutation of W56 to alanine substantially abrogates eIF4E affinity for both RTP and m^{7}GTP [7,9]. The ^{1}H-^{15}N HSQC of apo W56A eIF4E induces a large shift to F48, and only a minimal perturbation to N50 compared to wild-type eIF4E. Thus these residues, which may be considered as 'reporters' of high and low affinity complexes respectively, although close in sequence, can be differentially affected by both mutation and ligand binding.

Binding of RTP (at a 60-fold excess) to W56A eIF4E at high (50 μM) and low (2–5 μM) concentrations by NMR revealed different results. No significant changes compared to the wildtype spectra were evident from the high concentration titration (see Supplementary Fig. 2B, e.g. peaks N50 and T205 were similarly al-

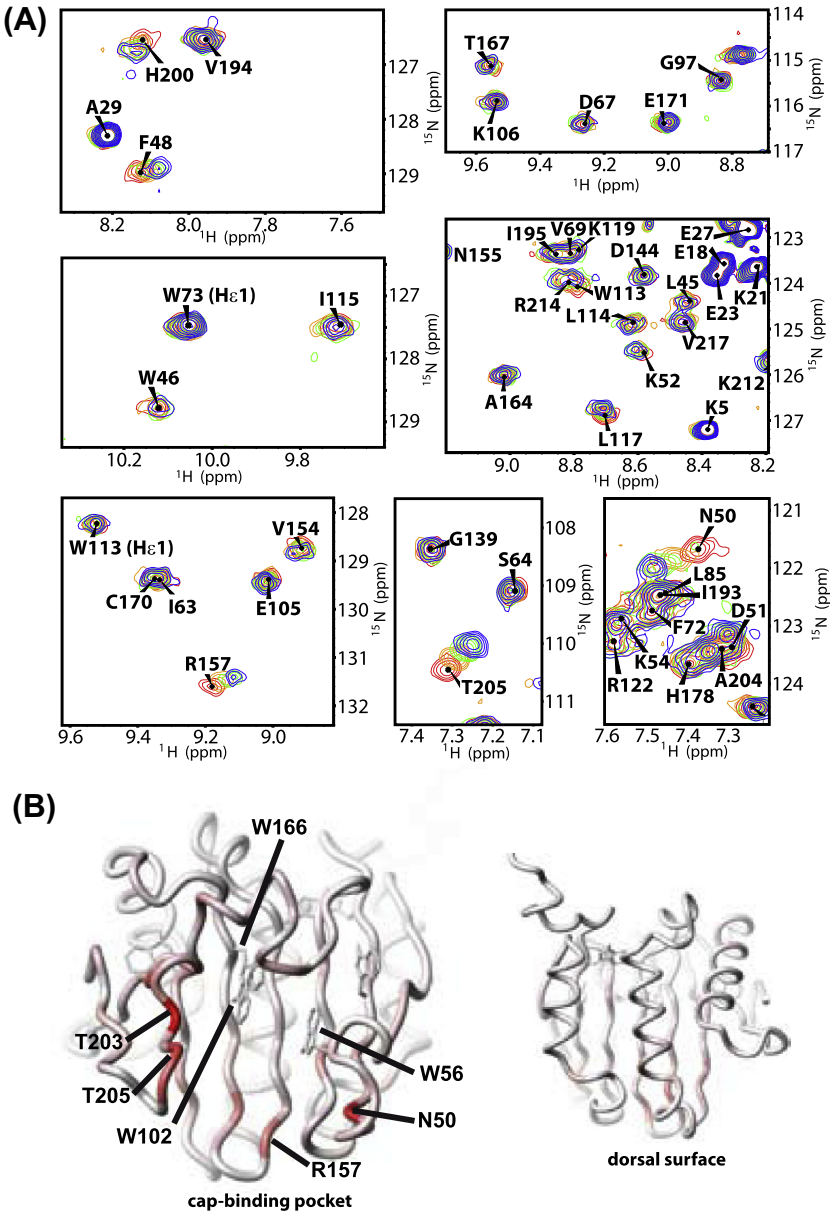

Fig. 3. NMR analysis of the high micromolar eIF4E-RTP complex is characterized by fast exchange. (A) ^{1}H–^{15}N HSQC spectra of 50 μM eIF4E (red) as a function of increasing concentration of RTP (up to 1:50; blue). The same regions as in Fig. 2A are shown. (B) ^{1}H-^{15}N HSQC chemical shift perturbations are mapped onto the eIF4E structure upon addition of RTP. Residues are color-coded according to the extent of chemical shift perturbation from white (no variation) to red (large variation). The same views as in Fig. 2B are shown.

tered in mutant and wildtype spectra). In contrast, at low eIF4E concentrations, RTP no longer bound eIF4E (Supplementary Fig. 2A). Thus W56 is only important for binding in the low concentration complexes, strongly supporting the notion that there are fundamental differences between the high and low concentration complexes. Significantly, the low concentration NMR complex has similar characteristics to the eIF4E–RTP complexes studied previously biophysically and in cells, such as high affinity and sensitivity to W56A, strongly suggesting this is the complex important for cellular function.

3.5. Comparison of conformational changes in the RTP- and m^{7}GTP–eIF4E complexes

Several crystal and NMR studies indicate that the m^{7}G cap intercalates between W56 and W102 with additional contacts made by E103, W166, and for the phosphates, K162 and R157 [4]. Consistent with binding at the cap site, all these residues are perturbed upon addition of RTP to eIF4E. Chemical shift perturbations of eIF4E upon binding of m^{7}GTP and RTP (at 2 μM eIF4E) are highlighted in Fig. 4B. Clearly a number of residues are similarly perturbed (colored in yellow), including F48 which undergoes among the largest shifts in both m^{7}GTP and RTP complexes. However, important differences are observed upon RTP binding. Notably, perturbations to the indole peaks of W56/102 were not as extensive which likely reflects the substantial differences in both size and charge between m^{7}GTP and RTP. Indeed there is substantial structural plasticity in the cap binding pocket as evidenced by high affinity binding of significantly bulkier ligands [17,18] and high *B*-factors for the W56/102 loops even when cap bound [5,19,20]. Thus, the lack of significant movement of the W56 and W102 indoles (note the W102 backbone amide is substantially af-

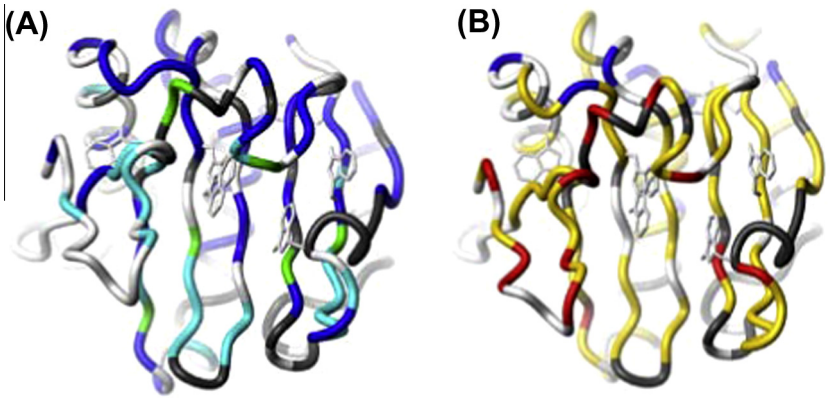

Fig. 4. Comparison of the residues affected in the RTP and m^7GTP eIF4E complexes. (A) Comparison of high and low affinity RTP complexes (low and high micromolar eIF4E samples, respectively). Results of spectral perturbations were mapped onto eIF4E cap bound structure. Color coding is as indicated: dark blue, change in high affinity complex relative to apo exclusively; light blue, change in both complexes relative to apo; green, change only in the low affinity complex relative to apo upon RTP binding; white, no change in either complex relative to apo; dark gray, unknown due to spectra overlap. (B) Comparison of high affinity RTP and m^7GTP complex, color-coding as above except for changes in both complexes relative to apo (yellow) and changes only in the m^7GTP complex relative to apo (red).

fected) upon RTP binding might reflect one or many of these mechanisms. It is possible that RTP binds deeper in the eIF4E pocket (given the effects on F48 and other nearby residues) and its smaller size allows the motions that are present in the apo eIF4E to persist, and of course, RTP could adopt multiple conformations in this pocket. Thus, for both cap binding and likely more so for RTP binding, there is likely substantial motion within the complexes.

Similar to m^7GTP binding to eIF4E, RTP induces substantial changes at the dorsal surface of eIF4E (Supplementary Fig. 3). These changes (which are important for increasing affinity for regulatory proteins [6,21–23]) are not identical to m^7GTP but are likely mediated via a similar allosteric path previously identified for eIF4E, e.g. via β-strands 5–6 to W130 on the internal face of helix 2 and adjacent residues lying on the dorsal surface, and in particular for a cluster comprising the residues H37, E40, V69 and D71. Notably we do not see any movement for W73 suggesting no involvement of the dorsal surface.

3.6. eIF4E concentration considerations

Our observations with RTP binding led us to examine whether the affinity of eIF4E for m^7GTP was similarly dependent on eIF4E concentration. Using ITC, we observe a steep concentration dependence with an affinity reduction of 8-fold in the range of 1.6–12.4 μM with stronger binding at low eIF4E concentrations (Supplementary Fig. 4B).

We hypothesized that reduced binding of eIF4E at higher concentration was due to aggregates. Consistently, we detected a concentration dependent aggregation of eIF4E using a variety of methods, including size exclusion chromatography (SEC), NMR self-diffusion and AUC (see Supplementary materials and Supplementary Fig. 4A and C). The results of the SEC showed only monomer at 0.5 μM eIF4E, with increasing amounts of aggregate (6%, 11% and 25%) at 2, 22 and 60 μM eIF4E, respectively. The aggregate eluted in the void volume, indicating a minimum molecular weight of 200 kDa. AUC data for 20 μM eIF4E estimated a molecular weight centered around 700 kDa with a very broad distribution indicating substantial heterogeneity (data not shown). Using SEC, we also observed time-dependent effect aggregation for the more concentrated eIF4E samples (60 μM) increasing from 25% to 50% aggregates after 3 days. In contrast, the low concentration samples (2–5 μM) showed no additional aggregation during even longer timeframes (data not shown). Thus, the concentration dependence on ligand affinity is not specific to RTP but appears related to the propensity of eIF4E to form very large aggregates.

Adding complexity to the system, guanosine analogs, which include ribavirin, are known to self-stack and in certain conditions can even form gels [24]. Using hydrophilic chromatography and mass spectrometry we detected an equimolar amount of dimer and monomer at 100 μM RTP and predominantly dimer (>98%) at 5 and 9 mM RTP.

Taken together, this strongly suggests that the active concentrations of both ligand and protein are lower than anticipated and account for some of the differences in affinity we observe as a function of eIF4E concentration. At very high concentrations of RTP, which would be typically used in NMR, the majority of RTP is dimer. We cannot rule out the presence of even higher aggregates that likely have poorer ionization efficiency than monomers and so the extent of aggregation for RTP reported here could well be an underestimate.

3.7. Ribavirin binds eIF4E in human cells

Ultimately, it is important to demonstrate that RTP interacts with eIF4E in human cells. RTP is not cell permeable and thus ribavirin, which is converted into RTP intracellularly [1] is used for these studies. From the clinical perspective, 20–40 μM ribavirin levels were routinely observed in AML patient plasma in the ribavirin monotherapy and ongoing ribavirin combination trials, and thus this concentration was used here [10,16] (see Supplementary methods). We observe a 6-fold enrichment of ^{3}H ribavirin in the eIF4E immunoprecipitations relative to controls indicating a strong interaction between eIF4E and RTP in cells consistent with the high affinity complexes we observe (Supplementary Fig. 5).

4. Discussion

Our NMR studies demonstrate that there are at least two modes for eIF4E binding to RTP dependent on concentration and likely driven by concentration dependent aggregation. Physically, both complexes utilize residues at or near to the cap-binding site, but the molecular contacts, relative binding affinity and sensitivity to the W56A mutation are distinct. The low concentration (2–5 μM) eIF4E-RTP complex exhibits similar high affinity binding and sensitivity to the W56A mutant as seen in previous biophysical studies[6,9,11]. Similar to m^7GTP binding, the low affinity RTP complex induced changes in the NMR spectrum at the dorsal sur-

face via an allosteric mechanism. However, we observe no changes to W73 consistent with previous studies showing mutation of W73 to alanine had no effect on RTP affinity for eIF4E [9]. The observation of a concentration dependent aggregation of eIF4E and concentration dependent affinity of eIF4E for RTP suggests these phenomena may be linked. A possible model for the observed binding is that aggregation at higher concentration obscures RTP from entering the cap binding pocket, and RTP-eIF4E association occurs at the surface loops, consistent with the large changes observed for N50, R167, T203 and T205; whereas at lower concentrations eIF4E is predominantly monomeric facilitating deeper access within the binding pocket.

The molecular details driving binding of RTP likely differ from m^7GTP. The cap-binding site is adjustable allowing for binding of cap-analogs with bulky substitutions, such as benzene in place of the methyl group on the guanosine ring where this actually increases affinity to eIF4E [18,25,26]. Similarly, eIF4E from nematodes binds both the mono- and trimethyl cap with similar affinity but mutation of E103 only impairs binding to monomethylated cap [26]. Taken together, these findings suggest that ligands can use different features to interact in eIF4E's cap-binding pocket. This is likely the case for RTP and m^7GTP. Further, given that RTP is much smaller than the cap, its precise position in the cap binding pocket may be more prone to "sliding" suggesting that there could be exchange within bound forms that could also contribute to the line broadening observed.

Our studies suggest that the high affinity/low concentration complex is the most physiologically relevant. For instance eIF4E is estimated to be present in the submicromolar range in cell lines [27], and ribavirin and thus RTP levels in patients are not typically more than 40 μM or so and certainly do not reach the millimolar level. The necessity of capturing the high affinity complex at low protein concentrations coupled with intermediate exchange phenomena, will make its structure determination particularly challenging. Given our biophysical studies at 0.2 μM eIF4E yield K_d's in the 0.17 μM range for RTP, it is likely that lowering concentrations in the NMR would lead to even tighter binding, but the technical limitations of collecting data on such dilute samples preclude such experiments. Notwithstanding, the clear differences in the binding site albeit within the cap-binding pocket, strongly suggest that these sorts of issues need to be considered for eIF4E drug design initiatives and also more generally as these phenomena are unlikely restricted to eIF4E. Further, a deeper understanding of multiple binding modes of eIF4E will be important in future drug design efforts.

Acknowledgments

We are grateful to Dr. Jack A. Kornblatt (CSFG and Department of Biology, Concordia University, Montreal) for carrying out ITC experiments. Studies were supported by NIH (RO1 98571). KLBB holds a Canada Research Chair. The Institute for Research in Immunology and Cancer receives support from the CIHR and FRSQ.

Appendix A. Supplementary data

Supplementary data associated with this article can be found, in the online version, at http://dx.doi.org/10.1016/j.bbrc.2013.03.125.

References

[1] K.L. Borden, B. Culjkovic-Kraljacic, Ribavirin as an anti-cancer therapy: acute myeloid leukemia and beyond?, Leuk Lymphoma 51 (2010) 1805–1815.
[2] B. Culjkovic, K.L. Borden, Understanding and targeting the eukaryotic translation initiation factor eIF4E in head and neck cancer, J. Oncol. 2009 (2009) 981679.
[3] W. Filipowicz, S.N. Bhattacharyya, N. Sonenberg, Mechanisms of post-transcriptional regulation by microRNAs: are the answers in sight?, Nat Rev. Genet. 9 (2008) 102–114.
[4] J. Marcotrigiano, A.C. Gingras, N. Sonenberg, et al., Cocrystal structure of the messenger RNA 5′ cap-binding protein (eIF4E) bound to 7-methyl-GDP, Cell 89 (1997) 951–961.
[5] K. Tomoo, Y. Matsushita, H. Fujisaki, et al., Structural basis for mRNA Cap-Binding regulation of eukaryotic initiation factor 4E by 4E-binding protein, studied by spectroscopic, X-ray crystal structural, and molecular dynamics simulation methods, Biochim. Biophys. Acta 1753 (2005) 191–208.
[6] L. Volpon, M.J. Osborne, I. Topisirovic, et al., Cap-free structure of eIF4E suggests a basis for conformational regulation by its ligands, EMBO J. 25 (2006) 5138–5149.
[7] N. Cohen, M. Sharma, A. Kentsis, et al., PML RING suppresses oncogenic transformation by reducing the affinity of eIF4E for mRNA, Embo J. 20 (2001) 4547–4559.
[8] J.R. Graff, B.W. Konicek, T.M. Vincent, et al., Therapeutic suppression of translation initiation factor eIF4E expression reduces tumor growth without toxicity, J. Clin. Invest. 117 (2007) 2638–2648.
[9] A. Kentsis, I. Topisirovic, B. Culjkovic, et al., Ribavirin suppresses eIF4E-mediated oncogenic transformation by physical mimicry of the 7-methyl guanosine mRNA cap, Proc. Natl. Acad. Sci. USA 101 (2004) 18105–18110.
[10] S. Assouline, B. Culjkovic, E. Cocolakis, et al., Molecular targeting of the oncogene eIF4E in AML: a proof-of-principle clinical trial with ribavirin, Blood 114 (2009) 257–260.
[11] A. Kentsis, L. Volpon, I. Topisirovic, et al., Further evidence that ribavirin interacts with eIF4E, RNA 11 (2005) 1762–1766.
[12] F. Pettersson, C. Yau, M.C. Dobocan, et al., Ribavirin treatment effects on breast cancers overexpressing eIF4E, a biomarker with prognostic specificity for luminal B-type breast cancer, Clin. Cancer. Res. 17 (2011) 2874–2884.
[13] T. Page, J.D. Connor, The metabolism of ribavirin in erythrocytes and nucleated cells, Int. J. Biochem. 22 (1990) 379–383.
[14] W.D. McCubbin, I. Edery, M. Altmann, et al., Circular dichroism and fluorescence studies on protein synthesis initiation factor eIF-4E and two mutant forms from the yeast Saccharomyces cerevisiae, J. Biol. Chem. 263 (1988) 17663–17671.
[15] T. von Der Haar, P.D. Ball, J.E. McCarthy, Stabilization of eukaryotic initiation factor 4E binding to the mRNA 5′-Cap by domains of eIF4G, J. Biol. Chem. 275 (2000) 30551–30555.
[16] S. Assouline, B. Kraljacic-Culjkovic, E. Cocolakis, et al., A Phase I combination study of ribavirin and low dose cytarabine arabinoside (ara-C) in M4/M5 acute myeloid leukemia (AML) and AML with high eIF4E, Blood (ASH Annual Meeting Abstracts) 118 (2011) 3606.
[17] X. Chen, D.J. Kopecky, J. Mihalic, et al., Structure-guided design, synthesis, and evaluation of guanine-derived inhibitors of the eIF4E mRNA-cap interaction, J. Med. Chem. 55 (2012) 3837–3851.
[18] C.J. Brown, I. McNae, P.M. Fischer, et al., Crystallographic and mass spectrometric characterisation of eIF4E with N7-alkylated cap derivatives, J. Mol. Biol. 372 (2007) 7–15.
[19] A. Niedzwiecka, J. Marcotrigiano, J. Stepinski, et al., Biophysical studies of eIF4E cap-binding protein: recognition of mRNA 5′ cap structure and synthetic fragments of eIF4G and 4E-BP1 proteins, J. Mol. Biol. 319 (2002) 615–635.
[20] J. Marcotrigiano, A.C. Gingras, N. Sonenberg, et al., Cap-dependent translation initiation in eukaryotes is regulated by a molecular mimic of eIF4G, Mol. Cell 3 (1999) 707–716.
[21] M. Ptushkina, T. von der Haar, M.M. Karim, et al., Repressor binding to a dorsal regulatory site traps human eIF4E in a high cap-affinity state, Embo J. 18 (1999) 4068–4075.
[22] M. Ptushkina, T. von der Haar, S. Vasilescu, et al., Cooperative modulation by eIF4G of eIF4E-binding to the mRNA 5′ cap in yeast involves a site partially shared by p20, Embo J. 17 (1998) 4798–4808.
[23] L. Volpon, M.J. Osborne, A.A. Capul, et al., Structural characterization of the Z RING-eIF4E complex reveals a distinct mode of control for eIF4E, Proc. Natl. Acad. Sci. USA 107 (2010) 5441–5446.
[24] W. Saenger, Principles of Nucleic Acid Structure, Springer-Verlag, New York, 1984.
[25] S.E. Carberry, E. Darzynkiewicz, J. Stepinski, et al., A spectroscopic study of the binding of N-7-substituted cap analogues to human protein synthesis initiation factor 4E, Biochemistry 29 (1990) 3337–3341.
[26] W. Liu, M. Jankowska-Anyszka, K. Piecyk, et al., Structural basis for nematode eIF4E binding an m(2,2,7)G-Cap and its implications for translation initiation, Nucleic Acids Res. 39 (2011) 8820–8832.
[27] M.J. Osborne, L. Volpon, J.A. Kornblatt, et al., EIF4E3 acts as a tumour suppressor by utilizing an atypical mode of methyl-7 guanosine cap recognition, Proc. Natl. Acad. Sci. USA (2013).
[28] A. Fukuyo, Y. In, T. Ishida, et al., Structural scaffold for eIF4E binding selectivity of 4E-BP isoforms: crystal structure of eIF4E binding region of 4E-BP2 and its comparison with that of 4E-BP1, J. Pept. Sci. 17 (2011) 650–657.